Observation of Coexisting Upflow and Downflow Hexagons in Boussinesq Rayleigh-Bénard Convection

Michel Assenheimer* and Victor Steinberg

Department of Physics of Complex Systems, The Weizmann Institute of Science, 76100 Rehovot, Israel

(Received 2 June 1995; revised manuscript received 16 October 1995)

We experimentally observed patterns consisting of domains of upflow hexagons coexisting with domains of downflow hexagons in Boussinesq Rayleigh-Bénard convection. The sequence of patterns, as the control parameter $\epsilon = \Delta T/\Delta T_c - 1$ is increased, is from ordered or disordered rolls at onset to extended targets and spirals at $\epsilon \sim 1$, to coexisting hexagons at $\epsilon \sim 3$. Hexagons occur for all values of the Prandtl number $2.8 \leq P \leq 28$ investigated. Surprisingly, they appear in a range where only rolls were known to be stable, and their wave number differs substantially from the roll wave number they coexist with.

PACS numbers: 47.54.+r, 47.20.Lz, 47.27.Te

One of the most intriguing recent discoveries in natural pattern formation in large aspect ratio Rayleigh-Bénard convection (RBC) is the observation of extended patterns [1–3] over a wide range of parameters where previously only rolls were known to be stable [4]. Subsequently, both numerical simulation of the generalized Swift-Hohenberg model [5] as well as integration of the full thermally driven Navier-Stokes equations in the Boussinesq approximation [6] accurately reproduced such spirals and targets. Although it has since been established that they are intrinsic to RBC, there is still little understanding why this state develops or of its dynamic behavior. Recently, Cross and Tu [7] introduced the notion of invasive defects as a first attempt to clarify the occurrence and characteristics of extended patterns. Driven by the difference in wave number selected by the focus and some background wave number, the defects expand to form spirals and targets, and eventually take over the entire system via their dynamics. Experimentally, a clear transition to the spiral-defect chaotic state was observed [8,9]. An obvious natural extension of these studies is the search for an upper stability limit of the spiral and the target chaotic state. In pursuing this goal we found that the extended pattern cores become unstable to defects of finite size and finite amplitude and of hexagonal symmetry. Surprisingly, upflow and downflow hexagons can coexist, and interesting instabilities of spiral and target cores can be observed.

In RBC hexagons occur as the first, subcritical bifurcation when the up-down symmetry is broken [4]. The most common causes for such a symmetry breaking are departures from the Boussinesq approximation (BA). They can be quantitatively estimated by the nondimensional parameter $Q = \sum_{i=0}^{4} \gamma_i p_i$, where the γ_i's are the nondimensional variations of density ρ, isobaric thermal expansion β_p, kinematic viscosity ν, thermal conductivity λ, and isobaric specific heat C_p with respect to the top and bottom temperatures, respectively, normalized by some reference value. The p_i's are linear functions of P^{-1} of $O(1)$ [4,10]. Here, $P = \nu/\kappa$ represents the Prandtl number and $\kappa = \lambda/\rho C_p$. Although the BA is valid for $Q^2 \ll R_c$ [4] (R_c is the critical value of the Rayleigh number, $R = \beta_p g d^3 \Delta T/\nu\kappa$, with d the fluid layer thickness and g the acceleration of gravity), at $Q \sim 1$ deviations from the BA are already quite significant [1,11]. The system then chooses either hexagons with upflow at the center (upflow hexagons) or hexagons with upflow at the boundaries (downflow hexagons), depending on the relative strength of the thermal properties of the fluid and boundaries, as well as the temperature dependence of various fluid properties.

Here, we report reentrant hexagonal patterns (i.e., not occurring near the threshold for convection) which appear via a core instability of spirals and targets in *Boussinesq* RBC. The most striking feature of these hexagonal planforms, however, is the fact that both upflow and downflow hexagons coexist simultaneously (see Fig. 1). Reentrant hexagons have first been observed in reaction-diffusion systems [12]. A recent theoretical study has revealed that both upflow and downflow hexagons can occur for different values of the control parameter [13]. In RBC in a planar liquid crystal with a nematic-isotropic

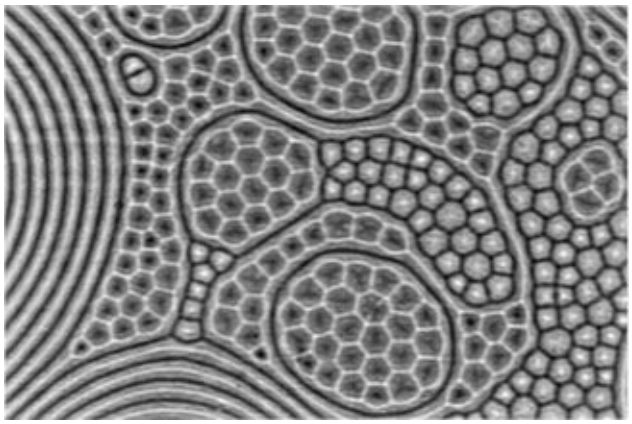

FIG. 1. Typical reentrant upflow and downflow hexagons. The parameters are $\epsilon = 3.4$, $P = 4.5$, and $Q = 0.16$.

 0031-9007/96/76(5)/756(4)$06.00

phase transition, reentrant hexagons of both types have also been found [14]. Coexistence, on the other hand, of upflow and downflow hexagons has been observed numerically by Hilali *et al.* in the generalized Swift-Hohenberg model with a large quadratic nonlinearity [15]. Recently, Dewel *et al.* found coexisting hexagonal patterns through coupling of a basic bifurcation with a zero mode [16]. Melo *et al.* found coexisting hexagons in the Faraday instability in a granular medium [17]. Experimentally, both reentrant and coexisting hexagons have been observed in the CIMA reaction [12,18].

We have studied RBC in SF_6 in the vicinity of the thermodynamical critical point. This allows us to vary the Prandtl number in a wide range and to achieve extremely large aspect ratios [19], while keeping Q negligibly small, as described elsewhere [1,3]. In particular, we showed previously that $\Delta T_c \sim \tau^{\gamma+\nu}$, $P \sim \tau^{-\nu}$, and $Q_c \sim \Delta T_c \tau \sim \tau^{\gamma+\nu-1}$, along the critical isochore. Here, ΔT_c represents the onset of convection, $\tau = (\overline{T} - T_c)/T_c$ is the reduced temperature, $\overline{T}$ and T_c ($T_c = 318.73$ K) are the average and critical temperatures, respectively, Q_c is the value of the non-Boussinesq parameter at onset, and $\gamma \approx 1.24$ and $\nu \approx 0.63$ are the critical exponents of the response and correlation functions, respectively. All the results presented below have been obtained in a cell of radial aspect ratio $\Gamma = D/2d = 80$, where D is the diameter, and thickness $d = 380$ μm. We varied the Prandtl number in the range $2.8 \leq P \leq 28$ by simply modifying the reduced temperature τ and the reduced density $\rho_r = \rho/\rho_c$ ($\rho_c = 730$ kg/m^3 is the critical density). The additional freedom in using off-critical densities allows to vary P while keeping ΔT_c fixed. Our choice of $d = 380$ μm stems from the compromise between the desire for a negligible value of Q_c, on the one hand, and the need for a detectable value of ΔT_c at the largest value of P (where ΔT_c is smallest), on the other hand. The largest value of $Q_c = 0.048$ occurred for the smallest value of $P = 2.8$. The thermodynamic and kinetic parameters needed to evaluate all relevant quantities will be published elsewhere [20].

Although hexagons appeared for all values of P in the range $2.8 \leq P \leq 28$, we will describe mainly the results of our most detailed study at $P = 4.5$. When the control parameter $\epsilon = \Delta T/\Delta T_c - 1$ is increased from zero the patterns found are nearly straight rolls over the entire cell (for large values of P domains of straight rolls are obtained [1]). At $\epsilon \lesssim 1$, a clear transition to extended patterns occurs [see Fig. 2(a)], as was recently investigated in detail [8,9]. It is quite likely that this transition is both aspect ratio and Prandtl number dependent. Consequently, we have determined the onset of the extended pattern state in the range $2.8 \leq P \leq 28$ for our cell of $\Gamma = 80$. The results are summarized in Table I and confirm that (i) the onset for extended patterns occurs for $\epsilon \lesssim 1$ [8,9], and (ii) non-Boussinesq behavior is irrelevant for the extended pattern state, as was previously implicitly assumed [6–9]. We would like to emphasize here again that our system is unique in that Q can be varied in an extremely wide range. In particular, extremely small values not only for $|Q|$ but also for $Q_{\text{abs}} = \sum_{i=0}^{4} |\gamma_i p_i|$ are readily obtained.

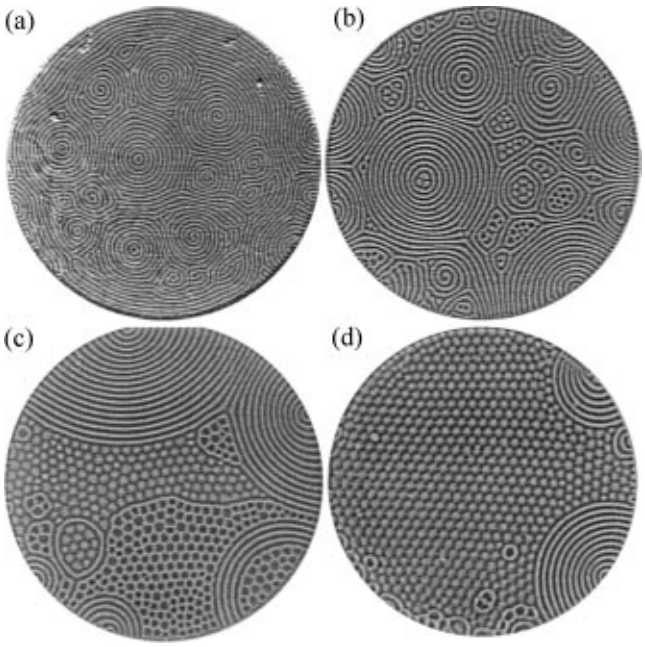

FIG. 2. Route to coexisting hexagons (ϵ, P, and Q are given in parentheses): (a) extended patterns (1.08, 9.8, 0.038); (b) onset of hexagons as core defects of extended patterns (2.74, 4.5, 0.14); (c) coexisting hexagons (3.4, 4.5, 0.16); (d) mainly one type of hexagon (4.2, 4.5, 0.19).

At $\epsilon = 2.74$ (for $P = 4.5$ and $Q = 0.138$ [21]), extended states become unstable to core defects whose sizes are of $O(d)$ [see Fig. 2(b)]. It can be seen that target cores are already unstable while spiral cores are not. Possibly at this value of P and ϵ spiral cores are more stable. It is obvious that the cores become unstable to defects of hexagonal symmetry when the focus selected wave number becomes small with respect to the average wave number.

TABLE I. The onsets of convection and of extended patterns and the non-Boussinesq parameter at the onset of extended pattern formation as a function of P.

P	τ ($\times 10^{-3}$)	ρ_r	ΔT_c (mK)	ΔT_c^{ext} (mK)	ϵ_{ext} $\frac{\Delta T_c^{\text{ext}}}{\Delta T_c} - 1$	$\lvert Q_{\text{ext}}\rvert$
2.8	31.9	1.306	143.8	270.7	0.882	0.086
4.3	28.6	1.160	46.4	85.7	0.845	0.025
5.0	28.5	1.028	23.0	43.1	0.873	0.045
9.7	15.6	1.028	8.8	18.3[a]	1.08[a]	0.037
24	6.43	1.028	3.3	13.8[a]	3.3[a]	0.061
28	4.25	1.028	1.0[b]	3.2	2.1	0.0061

[a]Possibly overestimated due to large $\Delta\epsilon$ used.
[b]Calculated from critical scaling; too small to be measured.

When the control parameter is increase slightly further to $\epsilon = 2.88$, spiral cores also become unstable. Figure 3 shows the typical dynamics of a spiral core close to the onset of its instability. Then, there are only few hexagons present in the core. The local core instability chooses either upflow or downflow hexagons.

Upon further increase of ϵ ($3 \lesssim \epsilon \lesssim 4$) the hexagonal core defects completely invade the system, mainly by cell division, as shown in Figs. 1 and 2(c). At this stage both interactions between upflow and downflow hexagons in the cores as well as in the bulk can be observed. Ising walls separate regions of upflow from domains of downflow. Although the dynamics is complex and the system never reaches a stationary state, it seems that Ising walls tend to straighten out by a phase jump mechanism. By shadowgraph microscopy, we observed that even in frustrated polygons angles of 120° are preserved.

A further increase to $4 \lesssim \epsilon \lesssim 5$ gives way to a pattern of preferably one type of hexagon. We have not verified whether this is due to a particular combination of P and ϵ. We have let the system equilibrate for as long as two horizontal diffusion times, but a completely defect free hexagonal lattice never formed [see Fig. 2(d)]. In particular, wall foci continued to form, whose cores usually became unstable to hexagonal defects. Remarkably, however, spontaneous formation of islands of single hexagons of the other type (and isolated rolls) always occurred. Often such a formation was induced by wave number gradients caused by various defects in the near vicinity.

At the largest values of P, where ΔT_c is small, we could easily reach the upper stability limit of the hexagonal patterns. In the range $\epsilon \gtrsim 15$, the pattern consisting mostly of spirals, targets, and hexagons becomes unstable to cross rolls, in agreement with Ref. [4], superimposing themselves onto the pattern. Their wave number is between ~3 and 6 times larger than the average wave number (see Fig. 4). It is interesting that the cross roll wave number is smallest midway between two extended pattern cores, while it is largest in their cores. At still higher ϵ a turbulent state free of any pattern is observed.

We have accurately measured the wave number in regions where large domains of rolls and hexagons coexist [e.g., Fig. 2(c)] by analyzing the azimuthally averaged structure function of the respective domains (see Fig. 5). By Gaussian fitting the peaks, we found $k_{\mathrm{roll}} = (1.89 \pm 0.24)d^{-1}$ (rolls only), while $k_{\mathrm{hex}} = (1.56 \pm 0.12)d^{-1}$ (both upflow and downflow hexagons). We have also separately determined the average wave number of upflow and downflow hexagons and found differences of at most 5%. By varying the focalization distance of the shadowgraph, we obtained a consistent wave number ratio of $k_{\mathrm{roll}}/k_{\mathrm{hex}} = 1.2$ to 1.3. Consequently, we argue that the differences in roll and hexagon wave numbers are not caused by shadowgraph nonlinearities. A direct fit of the azimuthally averaged structure function, using a sum of two Gaussians, averaged over 30 frames at $\epsilon = 3.4$, on the other hand, gives $k_{\mathrm{roll}} = (1.962 \pm 0.044)d^{-1}$ and $k_{\mathrm{hex}} = (1.561 \pm 0.038)d^{-1}$. Although we have no explanation, it is interesting to note that $k_{\mathrm{roll}}/k_{\mathrm{hex}} = \sqrt{3/2}$ to within about 2.5%, independent of ϵ, in accord with [22].

Since the observation of nonequilateral hexagons [12,18], recent theories have derived amplitude equations that allow for their existence, even within the BA [18,23–25]. We have Fourier transformed small regions of at least 60 hexagons (so that long wavelength curvature would not interfere) of Fig. 2(d) and found occasionally angular deviations between the peaks of 60.65° ± 0.20°, 60.60° ± 0.20°, and 58.75° ± 0.20°, respectively. Although this deviation from equilaterality is not as striking as in [18], it falls outside of our error bars. The regions of interest were always defect free, and the nearest

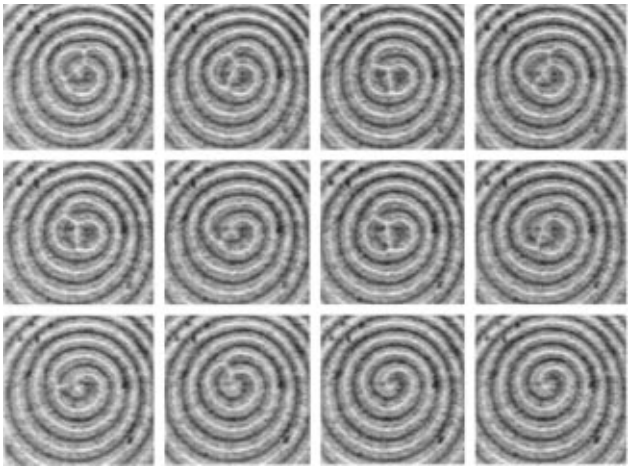

FIG. 3. A typical sequence showing the competition between hexagonal core defects and spirals near onset for hexagonal defects. The parameters are $\epsilon = 2.88$, $P = 4.5$, and $Q = 0.14$. Time progresses from left to right and top to bottom in steps of $2\tau_v$ (τ_v is the vertical diffusion time).

FIG. 4. Global cross rolls superimposed onto the basic pattern at $\epsilon = 22$ and $P = 17$.

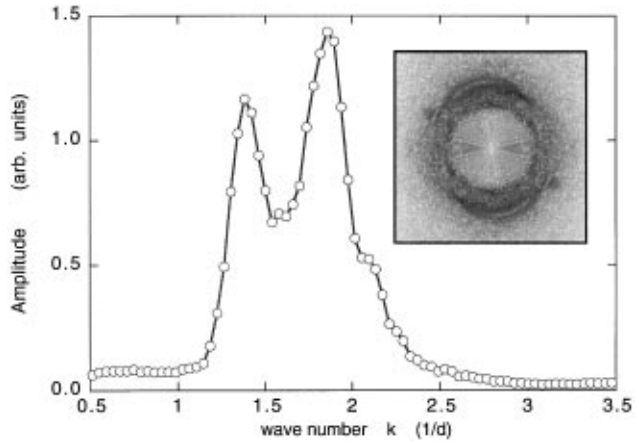

FIG. 5. The azimuthally averaged structure function of Fig. 2(b). The inset displays the structure function itself.

dislocations were at least several d away. Most regions of the pattern had peaks separated by $60.00° \pm 0.20°$, however.

In conclusion, we have studied large aspect ratio Boussinesq RBC, and for the first time observed the coexistence of domains of reentrant upflow and downflow hexagons. Just as for extended target and spiral states, the discovery of this state is particularly interesting, since it exists in a region where other structures were known to be stable [4]. The hexagons have a wave number that is substantially different from the average roll wave number they coexist with. A plausible explanation for the coexistence of upflow and downflow hexagons at higher values of the bifurcation parameter might be related to the coupling of the basic pattern to a zero mode, as suggested by a recent theory [16]. This zero k drifting mode could be caused by curved rolls, in particular at higher ϵ, even at large P. The observed ratio of roll to hexagon wave numbers, which agrees remarkably well with numerical simulations based on the model [22], strongly supports our suggestion.

This work was partially supported by the Minerva Foundation and the Minerva Center for Nonlinear Physics of Complex Systems. M. A. would like to acknowledge support from a Human Capital and Mobility fellowship. He profited from fruitful discussions with R. Hoyle, R. Zeitak, and particularly with P. Borckmans and G. Dewel.

*To whom correspondence should be addressed. Present address: Laboratoire de Physique Statistique, Ecole Normale Supérieure, 24 rue Lhomond, 75231 Paris Cedex 05, France. Electronic address: fnassen@physique.ens.fr

[1] M. Assenheimer and V. Steinberg, Phys. Rev. Lett. **70**, 3888 (1993).
[2] S. W. Morris, E. Bodenschatz, D. S. Cannell, and G. Ahlers, Phys. Rev. Lett. **71**, 2026 (1993).
[3] M. Assenheimer and V. Steinberg, Nature (London) **367**, 345 (1994).
[4] F. H. Busse, J. Fluid Mech. **30**, 625 (1967); Rep. Prog. Phys. **41**, 1929 (1978).
[5] H. Xi, J. D. Gunton, and J. Viñals, Phys. Rev. E **47**, R2987 (1993); Phys. Rev. Lett. **71**, 2030 (1993); M. Bestehorn, M. Fantz, R. Friedrich, and H. Haken, Phys. Lett. A **174**, 48 (1993).
[6] W. Decker, W. Pesch, and A. Weber, Phys. Rev. Lett. **73**, 648 (1994).
[7] M. C. Cross and Y. Tu, Phys. Rev. Lett. **75**, 834 (1995).
[8] Y. Hu, R. E. Ecke, and G. Ahlers, Phys. Rev. Lett. **74**, 391 (1995).
[9] M. Assenheimer, Ph.D. thesis, The Weizmann Institute of Science, 1994.
[10] It should be kept in mind that Q quantitatively estimates the effect of temperature dependent fluid properties in *incompressible* RBC. Compressibility which also causes deviations from the BA should be considered separately.
[11] E. Bodenschhatz, J. R. DeBruyn, G. Ahlers, and D. S. Cannell, Phys. Rev. Lett. **67**, 3078 (1991).
[12] Q. Ouyang and H. L. Swinney, Nature (London) **352**, 610 (1991); Chaos **1**, 411 (1991).
[13] J. Verdasca, A. De Wit, G. Dewel, and P. Borckmans, Phys. Lett. A **168**, 194 (1992); A. de Wit, Ph.D. thesis, Université Libre de Bruxelles, 1993.
[14] G. Ahlers, L. I. Berge, and D. S. Cannell, Phys. Rev. Lett. **70**, 2399 (1993); L. I. Berge, G. Ahlers, and D. S. Cannell, Phys. Rev. E **48**, R3236 (1993).
[15] M'F. Hilali, S. Métens, P. Borckmans, and G. Dewel, Phys. Rev. E **51**, 2046 (1995).
[16] G. Dewel, S. Métens, M'F. Hilali, P. Borckmans, and C. B. Price, Phys. Rev. Lett. **74**, 4647 (1995).
[17] F. Melo, P. B. Umbanhowar, and H. L. Swinney (to be published).
[18] G. H. Gunaratne, Q. Ouyang, and H. L. Swinney, Phys. Rev. E **50**, 2802 (1994).
[19] We have achieved aspect ratios as large as $\Gamma > 500$ in RBC with $d = 23$ μm very near the critical point.
[20] M. Assenheimer, A. Belmonte, A. Libchaber, and V. Steinberg (to be published).
[21] With the notation of Ref. [4], $10^3\gamma_i = 0.575$, -9.019, -0.140, -3.325, -13.913 and $P_i = 2.676$, -6.603, 2.755, 2.917, $-$ 6.229. Then $Q = 0.14$ and $Q_{\text{abs}} = 0.16$.
[22] M'F. Hilali, P. Borckmans, and G. Dewel (private communication).
[23] B. A. Malomed, A. A. Nepomnyashchy, and A. E. Nuz, Physica (Amsterdam) **70D**, 357 (1994).
[24] E. A. Kuznetsov, A. A. Nepomnyashchy, and L. M. Pismen (to be published).
[25] R. Hoyle, Ph.D. thesis, Cambridge University, 1994.